



Lower and upper bounds of quantum battery power in multiple central spin systems

Li Peng ^{1,2} Wen-Bin He,^{3,4,*} Stefano Chesi,^{3,5,4} Hai-Qing Lin,^{3,5} and Xi-Wen Guan ^{1,6,7,†}

¹State Key Laboratory of Magnetic Resonance and Atomic and Molecular Physics, Wuhan Institute of Physics and Mathematics, Innovation Academy for Precision Measurement Science and Technology, Chinese Academy of Sciences, Wuhan 430071, China

²University of Chinese Academy of Sciences, Beijing 100049, China

³Beijing Computational Science Research Center, Beijing 100193, China

⁴The Abdus Salam International Center for Theoretical Physics, Strada Costiera 11, 34151 Trieste, Italy

⁵Department of Physics, Beijing Normal University, Beijing 100875, China

⁶NSFC-SPTP Peng Huanwu Center for Fundamental Theory, Xian 710127, China

⁷Department of Theoretical Physics, Research School of Physics and Engineering, Australian National University, Canberra ACT 0200, Australia



(Received 10 January 2021; revised 17 April 2021; accepted 5 May 2021; published 28 May 2021)

We study the energy-transfer process in quantum battery systems consisting of multiple central spins and bath spins. Here with “quantum battery” we refer to the central spins, whereas the bath serves as the “charger.” For the single-central-spin battery, we analytically derive the time evolutions of the energy transfer and the charging power with arbitrary number of bath spins. For the case of multiple central spins in the battery, we find the scaling-law relation between the maximum power P_{\max} and the number of central spins N_B . It approximately satisfies a scaling law relation $P_{\max} \propto N_B^\alpha$, where scaling exponent α varies with the bath spin number N from the lower bound $\alpha = 1/2$ to the upper bound $\alpha = 3/2$. The lower and upper bounds correspond to the limits $N \rightarrow 1$ and $N \gg N_B$, respectively. In thermodynamic limit, by applying the Holstein-Primakoff transformation, we rigorously prove that the upper bound is $P_{\max} = 0.72BA\sqrt{NN_B^{3/2}}$, which shows the same advantage in scaling of a recent charging protocol based on the Tavis-Cummings model. Here B and A are the external magnetic field and coupling constant between the battery and the charger.

DOI: [10.1103/PhysRevA.103.052220](https://doi.org/10.1103/PhysRevA.103.052220)

I. INTRODUCTION

Energy resources are always an important subject of modern sciences [1], dating back to the fuel-coal energy to nuclear energy [2], to present renewable energy including wind and solar energy [1,3,4]. The exploitation of energy resources significantly involves the study of energy transfer, storage, and generation. Recently, it attracts enormous attention to study quantum heat engine [5,6] and refrigeration [7–10], energy storage and transfer in quantum-mechanical systems. The latter are named “quantum batteries” [11–25]. Classical electrical batteries store energy by electric field, which can be understood in the frame of electrodynamics. In contrast, the quantum battery usually refers to devices that utilize quantum degrees of freedom to store and transfer energy. In general, quantum degrees of freedom and their interplay can endow the quantum battery with advantages beyond the classical picture.

In the last few years, there have been a variety of methods to study the quantum battery, including realization schemes, battery power, and charging processes [26–32]. In these studies, quantum coherence and entanglement seemed to play a key role in the manipulation of quantum batteries. Alicki and Fannes [11] showed that entanglement can help extract more work in the charging process. However, the role of entanglement in work extraction is still in debate [12,13]. Ferraro *et al.*

[14] showed that the quantum advantage of charging power is manifested by an array of N collective two-level systems in a cavity in comparison with the N parallel quantum battery cells of the Dicke model. Andolina *et al.* [15] considered the role of correlations in different systems serving as a quantum battery, including the combination of two-level systems and quantum harmonic oscillators. There are also other schemes to realize quantum batteries, for example, using the open systems [33–38] and external field driving systems [39].

However, there still remain many open questions concerning quantum batteries. These mainly concern the battery’s largest energy, power, extractable energy, etc. First, the number of quantum battery cells cannot be increased to infinity in order to reach infinite power. Therefore it imposes a theoretical and practical challenge to manipulate as many quantum battery cells as possible due to the decoherent nature of quantum systems. Second, the number of quantum degrees of freedom in chargers is usually not big enough such that the transferred energy is not able to saturate the full cells of a battery during the charging process.

Nevertheless, both the numbers of quantum degrees of freedom and coupling strength between the battery and charger can alter the quality and power of the quantum battery.

This essentially involves the issue of how the storage capability of a quantum battery depends on the number of cells of both battery and charger.

In this paper, we study the energy-transfer process in quantum batteries of the multiple central spin model. Here the

*hewenbin18@csrc.ac.cn

†xwe105@wipm.ac.cn

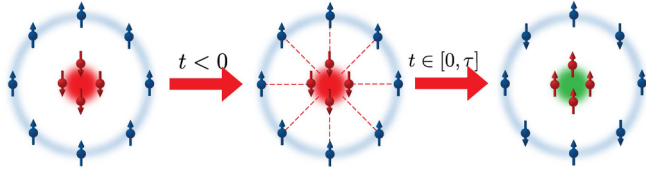


FIG. 1. The illustration of charging process of multiple central spin model working as quantum battery, whereas the bath spins serves as the charger. At $t < 0$, there is no interaction between battery and charger. While interaction is switched on during the charging process $t \in [0, \tau]$, the battery is charged.

battery consists of N_B spins which are displayed in collective mode during the charging process, whereas the charger has N bath spins; see Fig. 1. We analyze the dependence of the energy transfer and the power of the battery on the number N_B of battery spins and the number N of charger spins. We find that the transferred energy linearly increases with the number N_B of battery spins when N and N_B are comparable, then saturates to a certain value. The maximum power monotonically increases with respect to the number N_B in a power-law form $P_{\max} \propto N_B^\alpha$, where α shows a dependence on the number of charge spins N . For the limit $N \ll N_B$, the lower bound reads $\alpha = 1/2$. For the case $N \gg N_B$, the maximum energy of the battery always linearly increases with the number of battery spins. For $N \gg N_B$ and in the thermodynamic limit, the power-law relation of the maximum power $P_{\max} \rightarrow N_B^{1.5}$ is verified by numerical calculation. In the thermodynamic limit, using the Holstein-Primakoff transformation, we also rigorously prove that $P_{\max} = 0.72B(A\sqrt{NN_B}^\alpha)$, where the exponent gives the upper bound $\alpha = 3/2$. However, for N_B incoherent batteries with single spins, we prove that the maximum power is given by $P_{\max} \approx 0.72BA\sqrt{NN_B}$. Here B and A are respectively the external magnetic field and coupling constant between the battery and the charger. It turns out that the battery power essentially depends on the cell numbers of the battery and the charger. Our analytical results shed light on the high-power charging of quantum batteries.

II. THE QUANTUM BATTERY AND THE MODEL

Quantum battery. In this section, we discuss the basic setup of the quantum battery. The protocol of the underlying quantum battery consists of two parts: the quantum reservoir of energy-battery H_B and the energy charger H_C . Both the battery and charger are composed of quantum particles that have discrete energy levels and degeneracies. The charging process is accomplished by switching on the interaction H_I between the battery and the charger so as to complete the energy transfer; see Fig. 1. For this purpose, the whole Hamiltonian of this model is given by

$$H(t) = H_B + H_C + \lambda(t)H_I, \quad (1)$$

where coupling constant $\lambda(t)$ will be used to control the charging period. The coupling constant equals unity for one charging period $t \in [0, \tau]$ and is zero for other times. There exists energy input and output between the battery and charger during the charging period from $t = 0$ to $t = \tau$. The energy transfer, charging speed, and power of the battery essentially

depend on the number of batteries and chargers, the interaction strength between them, and other external drives if possible.

To comply with the terminology used in the previous works [14,15], we first introduce the definitions of energy and power of the quantum battery. We consider a system which evolves unitarily such that the wave function $\psi(t)$ describes the state of system. Meanwhile, the state of battery spins can be described by the reduced density matrix of the battery, $\rho_B(t) = \text{tr}_C[|\psi(t)\rangle\langle\psi(t)|]$, where tr_C denotes the trace over the spins in the charger. The energy of the battery is defined as the expectation value of the Hamiltonian H_B ,

$$E_B(t) = \text{tr}[H_B\rho_B(t)]. \quad (2)$$

Here ρ_B denotes the reduced density matrix of the battery. The transferred energy of the quantum battery is given by $\Delta E_B(t) = E_B(t) - E_B(0)$, where $E_B(0)$ is the energy before the charging process. Meanwhile, the charging power of the battery is defined as

$$P_B(t) = \Delta E_B(t)/t. \quad (3)$$

Since the unitary evolution of the whole system during the charging period, the energy will flow between charger and battery back and forth. It is not necessary to track the energy and power at every moment. Usually, one chooses the maximum energy as a measure of the capability for storing energy $E_{\max} = \max[\Delta E_B(t)]$, and accordingly the maximum power reads $P_{\max} = \max[P_B(t)]$.

It has been demonstrated [14] that collective battery cells of two-level systems coupled to a cavity mode can enhance the energy transfer by manipulating the detuning between the two-level systems and the cavity mode. They argue that the collective evolution proceeds through states characterized by quantum entanglement among the battery cells. In general, we naturally expect the existence of such a quantum advantage generated during the time evolution of the whole many-particle systems of the Hamiltonian (1). Here we aim to investigate the scaling laws of the maximum energy E_{\max} and the maximum power P_{\max} with respect to the numbers of battery spins. Similarly, in our work, the multiple central spins are prepared in a collective way, so that there also exists a certain form of quantum advantage in the system considered below. Such scaling laws reveal coherent nature between the battery and the charger, as well as the quantum entanglement among the spin qubits in the battery induced by the unitary evolution.

The model. To realize a high-power quantum battery, we consider the multiple central spin model with the Hamiltonian (1) given by

$$H_B = BS^z, \quad (4)$$

$$H_C = h\mathbf{J}^z, \quad (5)$$

$$H_I = A(\mathbf{S}^+\mathbf{J}^- + \mathbf{S}^-\mathbf{J}^+) + 2\Delta\mathbf{S}^z\mathbf{J}^z. \quad (6)$$

Here, for our convenience, we denote the large spin operators $\mathbf{S}^\alpha = \sum_{i=1}^{N_B} s_i^\alpha$, $\alpha = \{z, +, -\}$, and $\mathbf{J} = \sum_{j=1}^N \tau_j^\alpha$ for the battery and charger, respectively. We adopt different notations for central spins s_i^α and bath spins τ_j^α to avoid misunderstanding.

They are both the spin- $\frac{1}{2}$ operators. We regard the central spins as the storage cells of the quantum battery and the bath spins as charging energy carriers. The energy can be exchanged between the battery and the charger through the spin-exchange interaction term H_I , see also Fig. 1. H_I contains the spin flip-flop interaction and the Ising-type interaction, which are respectively denoted A and Δ , i.e., the exchange coupling constant and anisotropic parameter. We also set the coupling strength $A = 1$ for our rescaled units in the whole paper.¹ The parameters B and h are the effective external magnetic fields for the central spins and bath spins, respectively. N_B is the number of central spins, and N is the number of bath spins.

We introduce the Dicke state $|n\rangle = |\frac{N}{2}, n - \frac{N}{2}\rangle$, which is the eigenstate of \mathbf{J}^2 and \mathbf{J}^z . The Dicke state can be expressed as

$$|n\rangle = \frac{1}{\sqrt{C_N^n}} \sum_{j_1 < \dots < j_n} |j_1, \dots, j_n\rangle, \quad (7)$$

here $|j_1, \dots, j_n\rangle = \tau_{j_1}^+ \dots \tau_{j_n}^+ |\downarrow\rangle$, and the normalization coefficient C_N^n is a combination number $\frac{N!}{n!(N-n)!}$, and $|\downarrow\rangle$ denotes the down spins as the reference state. The Dicke state is a highly entangled many-body quantum state. The action of the above spin operators on state $|n\rangle$ are given by

$$\begin{aligned} \mathbf{J}^z |n\rangle &= \left(-\frac{N}{2} + n\right) |n\rangle, \\ \mathbf{J}^- |n\rangle &= \sqrt{b_{N,n}} |n-1\rangle, \\ \mathbf{J}^+ |n\rangle &= \sqrt{b_{N,n+1}} |n+1\rangle, \end{aligned}$$

where we denote the coefficient $b_{N,n} = n(N-n+1)$. For the large spin operator of the battery \mathbf{S} , they have similar properties through replacing N by N_B and replacing the spin operators τ_j^α by s_j^α , respectively. We consequently introduce the state basis of the whole system $|m, n\rangle$ for the degree of the battery $m \in \{0, 1, \dots, N_B\}$ and the degree of the charger $n \in \{0, 1, \dots, N\}$. The Hamiltonian of the whole system H can be diagonalized by the recurrence relation developed in Ref. [41]. For the special case $N_B = 1$, we can analytically obtain the whole dynamical evolution of spin polarization; see the Appendix.

III. NUMERICAL AND ANALYTICAL RESULTS

We first consider the numerical study of the general form of the quantum battery (1). We assume the initial state as

$$|\Phi_0\rangle = |\varphi_0\rangle_B \otimes |\phi_0\rangle_C. \quad (8)$$

Usually, the battery spins are in lowest states while the charger is in the higher excited states. For performing our numerical

¹For the unit of other parameters, we compared them with the A to obtain their units. At present, superconductor qubits may serve as quantum battery platforms to observe the results of this work since spin-exchange interactions can be realized experimentally. In a practical experiment, spin-exchange coupling usually takes the units time⁻¹, for instance, in Ref. [40], they set the Hamiltonian as H/\hbar and the spin-exchange coupling $J_{m,m+1} \approx 1/60 \text{ ns}^{-1}$.

study, we choose the initial state as $|\Phi_0\rangle = |0, N\rangle = |\downarrow, \uparrow\rangle$. The wave function of system evolves with time, namely,

$$|\psi(t)\rangle = \exp(-iHt)|\Phi_0\rangle. \quad (9)$$

By Eq. (2), we may calculate the evolution of the energy of battery as a function of time t .

A. Special case $N_B = 1$

At the beginning of this section, we first study the results of the special case $N_B = 1$ with $|\Phi_0\rangle = |\downarrow\rangle_B \otimes |\phi_0\rangle_C$ in order to get intuitive recognition of the energy transfer. Usually one can choose the states of bath spins as the Fock state or spin coherent state. Here we consider the Fock state for the initial state of the bath spins

$$|\Phi_0\rangle = |\downarrow\rangle \otimes |n\rangle, \quad (10)$$

where the bath spin state $|n\rangle$ represents n flipped spins among the N spins. The time evolution of the wave function can be obtained from the Hamiltonian H with Eqs. (4)–(6), i.e.,

$$|\psi(t)\rangle = e^{-i\theta t} [P_\uparrow^n(t) |\uparrow\rangle |n-1\rangle + P_\downarrow^n(t) |\downarrow\rangle |n\rangle]. \quad (11)$$

Here the global phase θ can be omitted and the two probability amplitudes are given by

$$P_\uparrow^n = -i \frac{2\sqrt{b_{N,n}}A}{\Omega_n} \sin\left(\frac{\Omega_n t}{2}\right)$$

and

$$P_\downarrow^n = i \frac{\Delta_n}{\Omega_n} \sin\left(\frac{\Omega_n t}{2}\right) + \cos\left(\frac{\Omega_n t}{2}\right).$$

The wave function satisfies the normalization condition $|P_\uparrow^n|^2 + |P_\downarrow^n|^2 = 1$. In the above equations, we denoted the parameters

$$\begin{aligned} \Delta_n &= B - h + (2n - 1 - N)\Delta, \\ \Omega_n &= \sqrt{\Delta_n^2 + 4b_{N,n}A^2}. \end{aligned}$$

Using the wave function (11), the charging energy and the power of quantum battery are obtained explicitly:

$$\Delta E_B(t) = B \frac{4b_{N,n}A^2}{\Omega_n^2} \sin^2\left(\frac{\Omega_n t}{2}\right), \quad (12)$$

$$P_B(t) = \Delta E_B(t)/t = B \frac{4b_{N,n}A^2}{\Omega_n^2 t} \sin^2\left(\frac{\Omega_n t}{2}\right). \quad (13)$$

The detailed calculation can be found in the Appendix, and see also the calculation for the Jaynes-Cummings (JC) model [15]. Based on this result, we briefly present a discussion on the energy transfer of the quantum battery below.

(i) Resonant case $B = h$, $\Delta = 0$, the charging energy is given by

$$\Delta E_B(t) = B \sin^2(\sqrt{b_{N,n}}At). \quad (14)$$

After an approximation, the maximum power is given by

$$P_{\max} \approx 0.72BA\sqrt{b_{N,n}}. \quad (15)$$

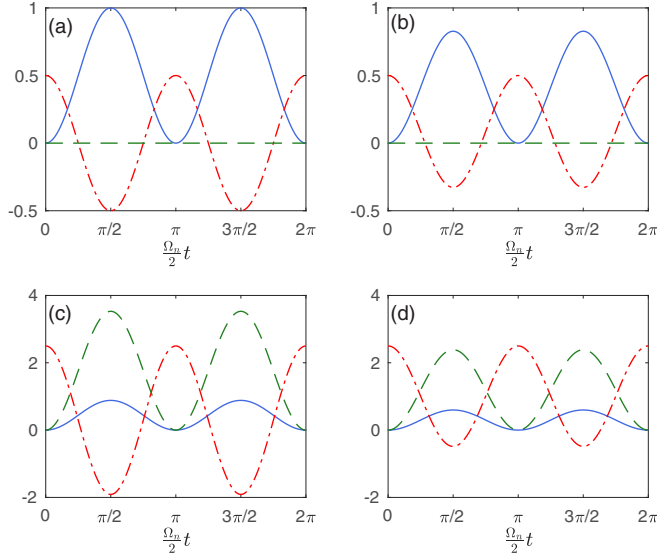


FIG. 2. The charging energy of quantum battery $\Delta E_B(t)$ (blue solid line), the energy of charger $\Delta E_C(t)$ (dashed red line), and the interaction energy $E_I(t)$ (dashed green line) are shown as function of $\Omega_n t/2$. (a) Charger and quantum battery are at resonance for $B = h = 1$ and $\Delta = 0$. (b) Charger and quantum battery are at resonance for $B = h = 1$ and $\Delta = 5$. (c) Charger and quantum battery are off resonance for $B = 5$, $h = 1$, and $\Delta = 0$. (d) Charger and quantum battery are off resonance for $B = 5$, $h = 1$, and $\Delta = 5$. In panels (a)–(d), we set $A = 1$, $N = 10$, and $n = N/2 = 5$. In panels (a) and (b), the interaction energy are always equal to zero for the whole time regime and the energy can be totally transferred from charger to battery.

From the expression of $\Delta E_B(t)$, the maximum transferred energy and the consumed time are given by

$$E_{\max} = B, \quad \tau_{\min} = \frac{\pi}{2A\sqrt{b_{N,n}}} \quad (16)$$

From the definition of $b_{N,n}$, we may obtain the minimum time to transfer the maximum energy, namely, $\tau_{\min} = \frac{\pi}{2A} \frac{1}{(N+1)/2}$, where we set $n = \frac{N+1}{2}$. This means that the quantum battery is able to store the maximum energy in the shortest time for the initial state with $n = (N+1)/2$ flipped bath spins.

(ii) Nonresonant case $B \neq h$ or $\Delta \neq 0$. In this case, we observe that the charging energy of quantum battery $|\Delta E_B(t)/B| < 1$ and interaction energy $E_I(t) = \langle H_I \rangle \neq 0$.

In Figs. 2(a) and 2(b), we show the results of the battery and charge at the resonance. There is no interaction energy between the battery and charger in Fig. 2(a). For Fig. 2(b), we chose $B = h$, $\Delta = 5$, $n = N/2 = 5$; the terms involving the factors $(N/2 - n)$ and $(B - h)$ in the charging energy of quantum battery vanish [see Appendix Eqs. (A7) and (A8)]. In this case, the maximum energy intake is limited by N due to conservation of energy. Figures 2(c) and 2(d) present the nonresonant case, for which there exists an interaction energy between the battery and charger. This indicates that the transferred energy from the charger to the quantum battery is essentially subject to the interaction form. In this scenario, the maximum transferred energy strongly depends on Δ , B , and h .

B. Arbitrary N_B case

For an arbitrary number N_B of battery spins, the eigenfunction is constructed by $|\varphi\rangle = \sum_m \sum_n c_{m,n} |m, n\rangle$. After substituting the above ansatz into the eigenvalue equation, the superposition coefficients $c_{m,n}$ are determined by the following recurrence equation:

$$w_{mn}c_{m,n} + A\sqrt{b_{N_B,m}b_{N,n+1}}c_{m-1,n+1} + A\sqrt{b_{N_B,m+1}b_{N,n}}c_{m+1,n-1} = Ec_{m,n}, \quad (17)$$

where the coefficient $b_{N_B,m} = m(N_B - m + 1)$ is defined as $b_{N,n}$ previously, and $w_{mn} = B(-\frac{N_B}{2} + m) + h(-\frac{N}{2} + n) + 2\Delta(-\frac{N_B}{2} + m)(-\frac{N}{2} + n)$. Here, for the battery, $m \in \{0, 1, \dots, N_B\}$ and for the charger $n \in \{0, 1, \dots, N\}$. However, the recurrence equation (17) with two variables m, n is very difficult to solve analytically. To study the energy transfer, we exactly diagonalize the Hamiltonian to obtain the time evolution of the system. Without losing the essential properties of the battery, we consider the interaction energy between charger and battery as zero by choosing the parameter $\Delta = 0$ and $B = h = 1$ in our numerical calculation. We show that, for this case, the Hamiltonian can map to the Tavis-Cummings model [42–44]. In addition, the system is prepared in the initial state $|\Phi_0\rangle = |\downarrow, \uparrow\rangle$, i.e., $m = 0$ and $n = N$. The time evolution of the energy and power of the battery can be obtained numerically and analytically.

For a classical battery device, the electric current is static so that a charging process can be complete in a certain time. However, for the quantum battery, the energy transfer is essentially subject to dynamical evolution and depends not only on the devices but also on the charging time. Let us first understand how the charging process depend on the number of the battery spins when the number of charger spins is fixed. If the battery spins are taken as the Fock state like that for the charger spins, the dynamical evolution of the battery involves the highly entangled Dicke state $|m\rangle$, $m = 1, \dots, N_B$ in charging process. Such a setting leads to a collective charging of the multiple central spin quantum battery, similar to the two-level system coupled to the single cavity mode, i.e., the Dicke model [14]. By using Holstein-Primakoff transformation, we prove that our model can be mapped to the Tavis-Cummings model, see Eq. (20) in the analytical study section. Meanwhile, the Tavis-Cummings model is related to the Dicke model by the rotating wave approximation, see Ref. [14]. Therefore, we naturally expect the existence of a general scaling relation between the battery power and the number of battery spins N_B in the quantum battery of the Tavis-Cummings-like model. After performing numerical calculations, we find that the maximum power takes the form

$$P_{\max} \propto \beta(N)N_B^\alpha, \quad (18)$$

where the exponent α is strongly affected by the number of charger spins and the initial state, while β is a function of the number of the charger spins N . Here the scaling exponent α essentially reflects the collective nature of the battery in transferring energy.

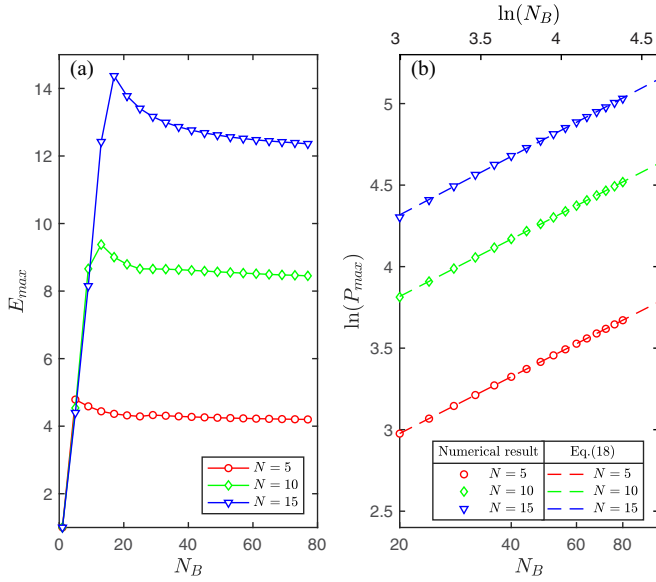


FIG. 3. The maximum (a) energy and (b) power of the multiple central spin model vs the number N_B of battery spins for different charger settings N . The dashed lines in panel (b) show the numerical fitting of the power relation (18) in a logarithmic scale for $N_B \in [20, 80]$, i.e., $N = 5$, $\alpha = 0.5013$, $\beta = 4.3706$ (red line); $N = 10$, $\alpha = 0.5067$, $\beta = 9.9668$ (green line), and $N = 15$, $\alpha = 0.5172$, $\beta = 15.9241$ (blue line), which agree with the numerical results shown in the corresponding symbols. This confirms the lower bound of the scaling exponent of the maximum power $\alpha \rightarrow 1/2$. Here we set $A = 1$, $B = h = 1$, $\Delta = 0$ with the initial state $n = N$, and $m = 0$.

1. For the case $N < N_B$

Using the above setting and initial state, i.e., $m = 0$, $n = N$, we first compute the time evolution of energy and maximum power. A more detailed explanation on the numerical calculation is given in the Appendix.

In Fig. 3, we show the maximum energy and maximum power as a function of the number N_B of battery spins for the different numbers of charger spins $N = 5$ (red circles), $N = 10$ (green squares), and $N = 15$ (blue triangles). In Fig. 3(a), we observe that the maximum energy E_{\max} varies with the number of battery spins $N_B \in [1, 80]$. The maximum energy increases linearly with respect to the number of battery spins N_B when $N_B \in [1, N]$ and saturates to a constant value when $N_B > N$. The maximum energy clearly shows a kink. In Fig. 3(b), we observe that the maximum power P_{\max} increases monotonically with respect to the battery spins N_B for different numbers of charger spins. The logarithmic plot of the maximum power P_{\max} directly gives the scaling exponent α which fits the relation (18) for the region $N_B \in [20, 80]$ and

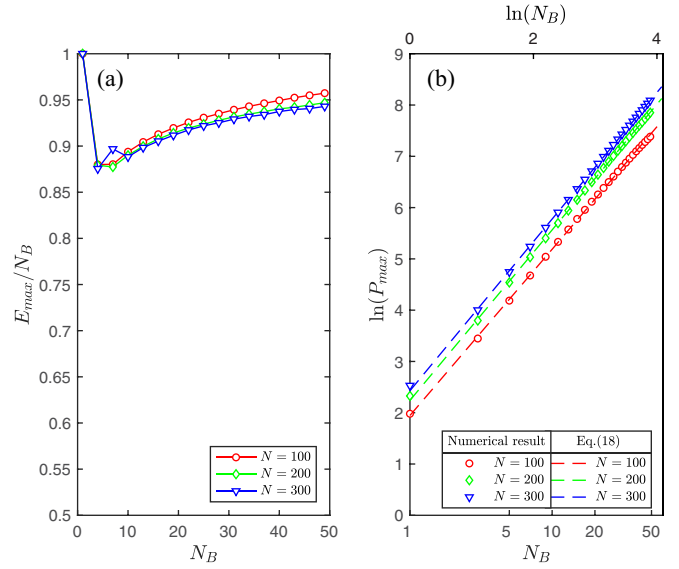


FIG. 4. The rescaled (a) maximum energy and (b) maximum power vs the number N_B of battery spins for different number N of charger spins. The dashed lines in panel (b) show the numerical fitting of the power relation (18) in logarithmic scale for $N_B \in [1, 50]$, i.e., $N = 100$, $\alpha = 1.4075$, $\beta = 7.0056$ (red line); $N = 200$, $\alpha = 1.4434$, $\beta = 9.4058$ (green line), and $N = 300$, $\alpha = 1.4540$, $\beta = 11.3456$ (blue line), which agree with the numerical results showing in the corresponding symbols. This agreement confirms the upper bound of the scaling exponent of the maximum power $\alpha \rightarrow 3/2$ in thermodynamic limit. Here we set $A = 1$, $B = h = 1$, $\Delta = 0$ with the initial state $n = N_B$, and $m = 0$.

$N_B > N$, see Fig. 3(b), Table I, and the Appendix. In Table I, we show the scaling exponent α and coefficient β for three different N , which confirm the lower bound of the scaling exponent of the maximum power, i.e., $\alpha \rightarrow 1/2$, in the region $N < N_B$.

2. For the case $N \gg N_B$

In Fig. 4, we demonstrate the maximum energy and the power-law relation (18) of the battery maximum power for $N \gg N_B$. Here, the number of quantum battery spins is $N_B \in [1, 50]$, and the number of charger spins is $N = 100$ (red circles), $N = 200$ (green squares), and $N = 300$ (blue triangles). We choose the initial state $n = N_B$ and $m = 0$, as suggested by the analytical result (31). We observe that the rescaled maximum energy E_{\max}/N_B does tend to saturate, see Fig. 4(a). Figure 4(b) shows a plot of the maximum power P_{\max} on a logarithmic scale. Numerical fitting indicates $\alpha \approx 1.45$. We observe that the numerical fit of the scaling exponent α with Eq. (18) is in good agreement with the analytical limit given in

TABLE I. The lower and upper bounds of the scaling exponent α obtained from numerical fitting of the Eq. (18) vs the number of charger cells N . For the upper bound, a comparison with the analytical result (31) in the thermodynamic limit is presented.

	Lower bound			Upper bound			Thermodynamic limit		
N	5	10	15	100	200	300	100	200	300
α	0.5013	0.5067	0.5172	1.4075	1.4434	1.4540	1.5	1.5	1.5
β	4.3706	9.9668	15.9241	7.0056	9.4058	11.3456	7.2	10.1823	12.4708

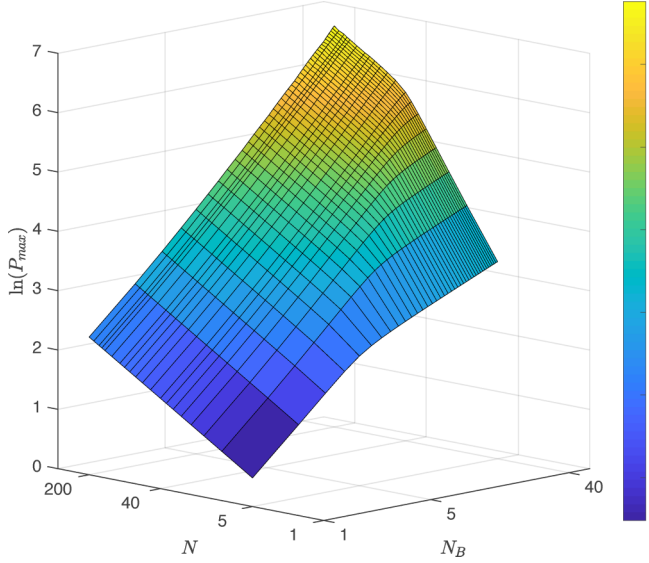


FIG. 5. Logarithmic contour plot of the maximum power vs the numbers of the battery spins N_B and charger spins N . It clearly shows different values of power scaling exponent α in the regimes $N < N_B$ and $N \gg N_B$. Here we set $A = 1$, $B = h = 1$, $\Delta = 0$ with the initial state $n = N$, and $m = 0$, and consider the ranges $N_B \in [1, 40]$ and $N \in [1, 200]$. However, in Fig. 4, the initial condition $n = N_B$ was used.

Eq. (31), as also seen in Table I. If N_B and N both take the thermodynamic limit, and $N \gg N_B$, the scaling exponent indeed approaches $\alpha \rightarrow 1.5$, which is consistent with the analytical result (31).

In Fig. 5, we further demonstrate the power-law relation (18) of the maximum power with respect to the numbers of battery spins N_B and charger spins N , where we set the initial state $n = N$ and $m = 0$ and consider the ranges $N_B \in [1, 40]$ and $N \in [1, 200]$.

This figure confirms the observations shown in Figs. 3 and 4. The plot of P_{\max} displays two clearly distinct planes separated by the condition $N = N_B$. For a fixed value of N , the slope of the down-turned plane reflects the value of α at $N < N_B$, whereas the slope of the upward plane indicates the value of α for the case $N \gg N_B$. It is worth noting that here we use the initial condition $n = N$, while in Fig. 4 $n = N_B$ was used.

Our numerical results show that the collective battery (multiple battery spins) enables the enhancement of the power through increasing the number of battery cells when the charger resources are large enough. This is quite in contrast with the single central spin battery, i.e., $N_B = 1$. In the next section, we present an analytical proof of these two bounds.

C. Analytical study

To get a comprehensive understanding of the lower and upper bounds of the scaling exponent found by numerics in the last section, we now present a rigorous calculation of the maximum energy and power of the quantum battery of Tavis-Cummings type. If we apply the Holstein-Primakoff transformation to both the bath and battery spins, the whole Hamiltonian of system (4)–(6) can be mapped to the Tavis-

Cummings model [42–44], where the N_B central spins are regarded as N_B two-level atoms.

For $N \gg 1$, $N_B \gg 1$, we apply transformation for charger spins

$$\begin{aligned} \mathbf{J}^+ &= \sqrt{N}a^\dagger \sqrt{1 - a^\dagger a/N}, \\ \mathbf{J}^- &= \sqrt{N}\sqrt{1 - a^\dagger a/N}a, \\ \mathbf{J}^z &= -\frac{N}{2} + a^\dagger a. \end{aligned} \quad (19)$$

Without losing generality, we can obtain the Tavis-Cummings model for the case $\Delta = 0$

$$H_{TC} = B\mathbf{S}^z + h\left(a^\dagger a - \frac{N}{2}\right) + A\sqrt{N}(\mathbf{S}^+ a + \mathbf{S}^- a^\dagger). \quad (20)$$

And we continue to apply the Holstein-Primakoff transformation to battery spins:

$$\begin{aligned} \mathbf{S}^+ &= \sqrt{N_B}b^\dagger \sqrt{1 - b^\dagger b/N_B}, \\ \mathbf{S}^- &= \sqrt{N_B}\sqrt{1 - b^\dagger b/N_B}b, \\ \mathbf{S}^z &= -\frac{N_B}{2} + b^\dagger b. \end{aligned} \quad (21)$$

In the above formulas, a (b) and a^\dagger (b^\dagger) both are annihilation and creation operators of bosons. Substituting Eqs. (19) and (21) into the Hamiltonian (4)–(6), we can obtain

$$\begin{aligned} H &\approx B\left(-\frac{N_B}{2} + b^\dagger b\right) + h\left(-\frac{N}{2} + a^\dagger a\right) \\ &\quad + A\sqrt{N_B N}(a^\dagger b + ab^\dagger). \end{aligned} \quad (22)$$

Here we neglected the terms $a^\dagger a/N$ and $b^\dagger b/N_B$ since $N \gg 1$, $N_B \gg 1$, while we set $\Delta = 0$ in the H_I to simplify our analytical study. Later, based on the whole Hamiltonian (22), we will analytically derive the scaling laws of the maximum energy and the maximum power with respect to the numbers of battery and charger spins. In this model, the total particle number is conserved and thus we have $[H, a^\dagger a + b^\dagger b] = 0$. Without losing a generality, we can choose a Hamiltonian of the following form for $B = h$:

$$H_I = A\sqrt{N_B N}(a^\dagger b + ab^\dagger). \quad (23)$$

We take the initial state as before: $|\Phi_0\rangle = |m, n\rangle = |m\rangle_B \otimes |n\rangle_C$, and the quantum battery is in the lowest state, namely, $m \rightarrow 0$. The maximum charging energy of the quantum battery is influenced not only by the energy levels of the battery and charger but also by the choice of their initial states. In quantum optics, the energy levels of photons can be infinite. For multiple central spins, the maximum transferred energy $\Delta E_B \propto BN_B$.

We reasonably choose $n - m \sim N_B$, i.e., the charger contains enough energy to charge the battery to a level of the maximum energy. The wave function at time t is given as the previous expression $|\psi(t)\rangle = \exp(-iH_I t)|\Phi_0\rangle$. By definition, the charging energy of the quantum battery is given by

$$\Delta E_B(t) = B[\langle \psi(t) | b^\dagger b | \psi(t) \rangle - \langle \Phi_0 | b^\dagger b | \Phi_0 \rangle]. \quad (24)$$

Let us further define the operator

$$\hat{\mathbf{F}} = b^\dagger b - a^\dagger a. \quad (25)$$

Its time evolution is given by

$$F(t) = \langle \Phi_0 | e^{iH_I t} \hat{\mathbf{F}} e^{-iH_I t} | \Phi_0 \rangle. \quad (26)$$

After carefully calculating the recurrent commutation relations between the operators H_I and $\hat{\mathbf{F}}$, we obtain the following expression:

$$\begin{aligned} e^{iH_I t} \hat{\mathbf{F}} e^{-iH_I t} &= \hat{\mathbf{F}} + \sum_n \frac{1}{n!} [iH_I t, [iH_I t, \dots, [iH_I t, \hat{\mathbf{F}}] \dots]] \\ &= \sum_{m=0}^{\infty} \frac{i^{2m+1}}{(2m+1)!} (2tA\sqrt{N_B N})^{2m+1} (a^\dagger b - ab^\dagger) \\ &\quad + \sum_{m=0}^{\infty} \frac{i^{2m}}{(2m)!} (2tA\sqrt{N_B N})^{2m} \hat{\mathbf{F}} \\ &= i \sin(2A\sqrt{N_B N}t) (a^\dagger b - ab^\dagger) \\ &\quad + \cos(2A\sqrt{N_B N}t) \hat{\mathbf{F}}. \end{aligned} \quad (27)$$

Substituting Eqs. (27) and (25) into Eq. (26), we further obtain the simple expression

$$F(t) = (m-n) \cos(2A\sqrt{N_B N}t). \quad (28)$$

Moreover, the total particle number $\hat{\mathbf{N}} = b^\dagger b + a^\dagger a$ is a conserved quantity, i.e., $[H_I, \hat{\mathbf{N}}] = 0$.

Therefore, we have $N(t) = \langle \psi(t) | \hat{\mathbf{N}} | \psi(t) \rangle = m+n$. It follows that

$$\begin{aligned} \langle \psi(t) | b^\dagger b | \psi(t) \rangle &= \frac{N(t) + F(t)}{2} \\ &= \frac{m+n}{2} + \frac{m-n}{2} \cos(2A\sqrt{N_B N}t). \end{aligned}$$

Thus, the charging energy and the power of the quantum battery are given by

$$\Delta E_B(t) = B(n-m) \sin^2(A\sqrt{N_B N}t), \quad (29)$$

$$P_B(t) = B(n-m) \frac{\sin^2(A\sqrt{N_B N}t)}{t}, \quad (30)$$

respectively.

It is straightforward to obtain the maximum power that is given by $P_{\max} = B0.72A\sqrt{N_B N}(n-m)$ for a time $\tau = 1.16/(A\sqrt{N_B N})$.

As mentioned in the previous section, we demand $n-m \sim N_B$ and $N \gg N_B$, thus the maximum power is given by

$$P_{\max} = 0.72BA\sqrt{N}N_B^{3/2}, \quad (31)$$

which reveals a significant advantage of this charging protocol, leading in turn to the upper bound of the scaling exponent $\alpha = 3/2$. We observe that, in the early charging process, the power reaches the maximum whereas the energy does not reach the maximum. This means that the maximum power $P_{\max} \propto N_B^{3/2}$ can indeed occur in the early time of the charging process, when the flipped spin $\langle b^\dagger b \rangle$ in the battery is much less than the number N_B of battery cells. Therefore the Holstein-Primakoff transformation is valid for our analytical results.

On the other hand, for the limit $N \rightarrow 1$, the maximum power shows a lower bound of such advantage, see Fig. 3(b). The evolution of the system can be easily obtained for $N = 1$ with the initial state $|m, \uparrow\rangle$. The energy $\Delta E_B =$

$B \sin^2(\sqrt{b_{N_B, m+1}} At)$ and power $P_B = B \sin^2(\sqrt{b_{N_B, m+1}} At)/t$, so that the maximum of the power is given by $P_{\max} \approx 0.72B\sqrt{b_{N_B, m+1}}A$ for the charging time $1.16/\sqrt{b_{N_B, m+1}}A$. According to the previous setting, the initial state of the battery spins are in the lowest state $m \rightarrow 0$, which gives $\sqrt{b_{N_B, m+1}} = \sqrt{N_B}$ and leads to $P_{\max} \propto \sqrt{N_B}$. This is consistent with the numerical result given in Fig. 3(b), i.e., the scaling exponent α varies from the lower bound $\alpha = 1/2$ to the upper bound $3/2$ when the number of charger spins N changes from small to the thermodynamic limits, i.e., $N \gg 1$ and $N_B \gg 1$, while the condition $N \gg N_B$ holds.

IV. CONCLUSION

We have studied numerically and analytically the high-power quantum battery through the multiple central spin model. The advantage of a quantum battery has been demonstrated through the maximum power of the quantum battery $P_{\max} = 0.72BA\sqrt{N}N_B^\alpha$ that exhibits a universal power-law dependence of the battery cells (spins) under the condition $N_B \ll N$. Such a power-law relation is analytically derived by the quantum battery of the Tavis-Cummings type. We have also observed that the power-law exponent of the battery power depends on the number N of charger spins, namely, the scaling exponent α varies with the bath-spin number N from the lower bound $\alpha = 1/2$ to the upper bound $\alpha = 3/2$. From the maximum power (15) of the single central spin battery, we see clearly the maximum power of N_B incoherent quantum batteries of single central spin systems is given by $P_{\max} \approx 0.72BA\sqrt{N}N_B$. Therefore, a quantum advantage is revealed from the maximum power (31) of the quantum battery of N_B central spins. In the latter case, coherence of the N_B central spins is naturally created by the interaction between the battery and charger spins. In the Appendix, we present the analytical results of the quantum battery with $N_B = 1$ and an introduction to our numerical method. Our results display the role of how both the charger and battery are capable of enhancing the quantum advantage of Tavis-Cummings-type systems. Our rigorous results of dynamical energy transfer shed light on the design of quantum batteries.

ACKNOWLEDGMENTS

W.-B.H. acknowledges support from NSAF (Grant No. U1930402). X.-W.G. is supported by the NSFC Grant No. 11874393, and the National Key R&D Program of China No. 2017YFA0304500. S.C. acknowledges support from NSFC (Grants No. 11974040 and No. 1171101295) and the National Key R&D Program of China No. 2016YFA0301200. W.-B.H., S.C., and H.-Q.L. acknowledge financial support from NSAF U1930402 and computational resources from the Beijing Computational Science Research Center. W.-B.H. and H.-Q.L. also acknowledge support from NSFC 12088101.

APPENDIX A: THE EXPLICIT FORMS OF THE CHARGING ENERGY

For the special case $N_B = 1$, the Hamiltonian can be written as a 2×2 matrix in the bases $|\downarrow\rangle|n\rangle, |\uparrow\rangle|n-1\rangle$, where

$n = 1, 2, \dots, N$,

$$H_n = \begin{pmatrix} \frac{B-h}{2} + (n-1-N/2)\Delta & \sqrt{b_{N,n}}A \\ \sqrt{b_{N,n}}A & -\frac{B-h}{2} - (n-N/2)\Delta \end{pmatrix}. \quad (\text{A1})$$

It is easy to diagonalize above small matrix H analytically to obtain the evolution operator $U(t) = \exp(-iHt)$. The wave function can be derived by $|\psi(t)\rangle = U(t)|\Phi_0\rangle$. The Hamiltonian can be written as $H_n = (\Delta_n/2)\hat{\sigma}_z + \sqrt{b_{N,n}}A\hat{\sigma}_x + C$, here C is constant. The evolution operator $U(t)$ can be obtained by using property of Pauli matrix namely $\exp(i\theta\hat{n}\cdot\hat{\sigma}) = \cos(\theta)I + i\sin(\theta)\hat{n}\cdot\hat{\sigma}$. It is $U(t) = \cos(\Omega_n t/2)I - i\sin(\Omega_n t/2)[(\Delta_n/\Omega_n)\hat{\sigma}_z + 2(\sqrt{b_{N,n}}A/\Omega_n)\hat{\sigma}_x]$, where

$$\Delta_n = B - h + (2n - 1 - N)\Delta, \\ \Omega_n = \sqrt{\Delta_n^2 + 4b_{N,n}A^2}.$$

By acting with the evolution operator $U(t)$ on the initial state $|\downarrow\rangle|n\rangle$, we finally obtain the time-dependent wave function.

We explicitly rewrite the wave function for the $N_B = 1$ case (11) as

$$|\psi(t)\rangle = e^{-i\theta t}[P_{\uparrow}^n(t)|\uparrow\rangle|n-1\rangle + P_{\downarrow}^n(t)|\downarrow\rangle|n\rangle]. \quad (\text{A2})$$

Here the global phase θ can be omitted and the two amplitudes are given by

$$P_{\uparrow}^n(t) = -i\frac{2\sqrt{b_{N,n}}A}{\Omega_n} \sin\left(\frac{\Omega_n t}{2}\right), \\ P_{\downarrow}^n(t) = i\frac{\Delta_n}{\Omega_n} \sin\left(\frac{\Omega_n t}{2}\right) + \cos\left(\frac{\Omega_n t}{2}\right).$$

The wave function satisfies the normalization condition, namely, $|P_{\uparrow}^n(t)|^2 + |P_{\downarrow}^n(t)|^2 = 1$. And the parameters are denoted $\Delta_n = B - h + (2n - 1 - N)\Delta$, $\Omega_n = (\Delta_n^2 + 4b_{N,n}A^2)^{1/2}$. The density matrix for the system can be obtained as

$$\rho(t) = |\Psi(t)\rangle\langle\Psi(t)| \\ = P_{\uparrow}^n(t)P_{\uparrow}^n(t)^*|\uparrow\rangle|n-1\rangle\langle\uparrow| + P_{\uparrow}^n(t)P_{\downarrow}^n(t)^*|\uparrow\rangle|n-1\rangle\langle\downarrow| \\ + P_{\downarrow}^n(t)P_{\uparrow}^n(t)^*|\downarrow\rangle|n\rangle\langle\uparrow| + P_{\downarrow}^n(t)P_{\downarrow}^n(t)^*|\downarrow\rangle|n\rangle\langle\downarrow|. \quad (\text{A3})$$

Then the reduced density matrices ρ_B and ρ_C are given respectively as

$$\rho_B(t) = \text{tr}_C[|\Psi(t)\rangle\langle\Psi(t)|] \\ = P_{\uparrow}^n(t)P_{\uparrow}^n(t)^*|\uparrow\rangle\langle\uparrow| + P_{\downarrow}^n(t)P_{\downarrow}^n(t)^*|\downarrow\rangle\langle\downarrow|, \quad (\text{A4})$$

$$\rho_C(t) = \text{tr}_B[|\Psi(t)\rangle\langle\Psi(t)|] \\ = P_{\uparrow}^n(t)P_{\uparrow}^n(t)^*|n-1\rangle\langle n-1| + P_{\downarrow}^n(t)P_{\downarrow}^n(t)^*|n\rangle\langle n|. \quad (\text{A5})$$

After some simple algebra, we derive the energy of the quantum battery, the energy of charger, and the energy of interaction between charger and battery by substituting the above density matrix into the definition (2):

$$E_B(t) = \text{tr}[H_B\rho_B(t)] = B\left[\frac{4b_{N,n}A^2}{\Omega_n^2} \sin^2\left(\frac{\Omega_n t}{2}\right) - \frac{1}{2}\right], \quad (\text{A6})$$

$$E_C(t) = \text{tr}[H_C\rho_C(t)] = h\left[\left(-\frac{N}{2} + n\right) - \frac{4b_{N,n}A^2}{\Omega_n^2} \sin^2\left(\frac{\Omega_n t}{2}\right)\right], \quad (\text{A7})$$

$$E_I(t) = \text{tr}[H_I\rho(t)] = \Delta\left(\frac{N}{2} - n\right) - (B - h)\frac{4b_{N,n}A^2}{\Omega_n^2} \sin^2\left(\frac{\Omega_n t}{2}\right). \quad (\text{A8})$$

APPENDIX B: EXACT DIAGONALIZATION AND FITTING THE SCALING LAW

In this Appendix, we present in details the exact diagonalization method. According to the action of larger spin operator on the Dicke state, we have

$$\mathbf{J}^z|n\rangle = \left(-\frac{N}{2} + n\right)|n\rangle, \quad (\text{B1})$$

$$\mathbf{J}^-|n\rangle = \sqrt{b_{N,n}}|n-1\rangle, \quad (\text{B2})$$

$$\mathbf{J}^+|n\rangle = \sqrt{b_{N,n+1}}|n+1\rangle, \quad (\text{B3})$$

such that J^z, J^-, J^+ are written as $(N+1) \times (N+1)$ matrix, for example, and J^z and J^- are given by

$$(J^z)_{mn} = \begin{cases} \left(-\frac{N}{2} + n\right), & \text{for } m = n \\ 0, & \text{for others,} \end{cases} \quad (\text{B4})$$

and

$$(J^-)_{mn} = \begin{cases} \sqrt{b_{N,n}}, & \text{for } m = n-1 \\ 0, & \text{for others,} \end{cases} \quad (\text{B5})$$

respectively. At the same time, the operators S^z, S^-, S^+ can be written as $(N_B+1) \times (N_B+1)$ matrices, too. By combining the matrices J and S , we obtain the matrix form of the whole Hamiltonian (4)–(6). Thus the dimension of the Hamiltonian in the Dicke basis is $(N_B+1)(N+1)$. For $N_B \leq 50$, and

$N \leq 300$, the Hamiltonian can be diagonalized directly to obtain the evolving operator $U(dt) = \exp(-iHdt)$ with suitable time step dt .

The time-dependent wave function can be obtained numerically $|\psi(t)\rangle = U(dt) \cdots U(dt)|\Phi_0\rangle$. Then, according to Eqs. (2) and (3), the energy and power can be computed.

Scaling relation

The scaling relation of the maximal power of battery reads

$$P_{\max} \propto \beta(N)N_B^\alpha. \quad (\text{B6})$$

By taking the logarithm, we use linear fitting to obtain the scaling exponent α

$$\ln(P_{\max}) = \alpha \ln(N_B) + \ln(\beta(N)), \quad (\text{B7})$$

where β is a constant for a fixed N . Since the total energy is conserved, the energy reaches a saturation point for $N_B \geq N$, see Fig. 3(a). Therefore we used the data after the saturation point to fit the scaling relation (B7) within the region $N_B \in [20, 80]$ in Fig. 3(b). Whereas, for the case $N \gg N_B$, we fit the scaling relation (B7) for the region $N_B \in [1, 50]$ and $N \gg N_B$ in Fig. 4(b). We find that it agrees with our analytical relation (31) in the thermodynamic limit; see the main text.

-
- [1] Electricity Generation by Source (International Energy Agency), <https://www.iea.org/>.
- [2] G. Gamow, *Phys. Rev.* **53**, 595 (1938).
- [3] D. Gielen, F. Boshell, and D. Saygin, *Nat. Mater.* **15**, 117 (2016).
- [4] J. W. Agerl, A. A. Lapkin, *Science* **360**, 707 (2018).
- [5] P. Medley, D. M. Weld, H. Miyake, D. E. Pritchard, and W. Ketterle, *Phys. Rev. Lett.* **106**, 195301 (2011).
- [6] Y.-Y. Chen, G. Watanabe, Y.-C. Yu, X.-W. Guan, A. del Campo, *npj Quantum Inf.* **5**, 88 (2019).
- [7] D. M. Weld, H. Miyake, P. Medley, D. E. Pritchard, and W. Ketterle, *Phys. Rev. A* **82**, 051603(R) (2010).
- [8] Y.-C. Yu, S. Zhang, and X.-W. Guan, *Phys. Rev. Res.* **2**, 043066 (2020).
- [9] L. Peng, Y. Yu, and X.-W. Guan, *Phys. Rev. B* **100**, 245435 (2019).
- [10] B. Wolf, Y. Tsui, D. Jaiswal-Nagar, U. Tutsch, A. Honecker, K. Remović-Langer, G. Hofmann, A. Prokofiev, W. Assmus, G. Donath, and M. Lang, *Proc. Natl. Acad. Sci. USA* **108**, 6862 (2011).
- [11] R. Alicki and M. Fannes, *Phys. Rev. E* **87**, 042123 (2013).
- [12] K. V. Hovhannisyán, M. Perarnau-Llobet, M. Huber, and A. Acín, *Phys. Rev. Lett.* **111**, 240401 (2013).
- [13] F. Campaioli, F. A. Pollock, F. C. Binder, L. Céleri, J. Goold, S. Vinjanampathy, and K. Modi, *Phys. Rev. Lett.* **118**, 150601 (2017).
- [14] D. Ferraro, M. Campisi, G. M. Andolina, V. Pellegrini, and M. Polini, *Phys. Rev. Lett.* **120**, 117702 (2018).
- [15] G. M. Andolina, D. Farina, A. Mari, V. Pellegrini, V. Giovannetti, and M. Polini, *Phys. Rev. B* **98**, 205423 (2018).
- [16] F. Campaioli, F. A. Pollock, and S. Vinjanampathy, in *Thermodynamics in the Quantum Regime, Fundamental Theories of Physics*, edited by F. Binder, L. Correa, C. Gogolin, J. Anders, and G. Adesso (Springer, Cham, 2018), Vol. 195.
- [17] T. P. Le, J. Levinsen, K. Modi, M. M. Parish, and F. A. Pollock, *Phys. Rev. A* **97**, 022106 (2018).
- [18] S. Julià-Farré, T. Salamon, A. Riera, M. N. Bera, and M. Lewenstein, *Phys. Rev. Res.* **2**, 023113 (2020).
- [19] D. Rossini, G. M. Andolina, and M. Polini, *Phys. Rev. B* **100**, 115142 (2019).
- [20] G. M. Andolina, M. Keck, A. Mari, V. Giovannetti, and M. Polini, *Phys. Rev. B* **99**, 205437 (2019).
- [21] F. Caravelli, G. C.-D. Wit, L. P. García-Pintos, and A. Hamma, *Phys. Rev. Res.* **2**, 023095 (2020).
- [22] G. M. Andolina, M. Keck, A. Mari, M. Campisi, V. Giovannetti, and M. Polini, *Phys. Rev. Lett.* **122**, 047702 (2019).
- [23] L. P. García-Pintos, A. Hamma, and A. del Campo, *Phys. Rev. Lett.* **125**, 040601 (2020).
- [24] A. C. Santos, *Phys. Rev. E* **103**, 042118 (2021).
- [25] F. H. Kamin, F. T. Tabesh, S. Salimi, and Alan C. Santos, *Phys. Rev. E* **102**, 052109 (2020).
- [26] F. Pirmoradian and K. Mølmer, *Phys. Rev. A* **100**, 043833 (2019).
- [27] Y.-Y. Zhang, T.-R. Yang, L. Fu, and X. Wang, *Phys. Rev. E* **99**, 052106 (2019).
- [28] S.-Y. Bai and J.-H. An, *Phys. Rev. A* **102**, 060201(R) (2020).
- [29] D. Rossini, G. M. Andolina, D. Rosa, M. Carrega, and M. Polini, *Phys. Rev. Lett.* **125**, 236402 (2020).
- [30] A. C. Santos, B. Çakmak, S. Campbell, and N. T. Zinner, *Phys. Rev. E* **100**, 032107 (2019).
- [31] A. C. Santos, A. Saguia, and M. S. Sarandy, *Phys. Rev. E* **101**, 062114 (2020).
- [32] N. Friis and M. Huber, *Quantum* **2**, 61 (2018).
- [33] S. Gherardini, F. Campaioli, F. Caruso, and F. C. Binder, *Phys. Rev. Res.* **2**, 013095 (2020).
- [34] M. Carrega, A. Crescente, D. Ferraro, and M. Sassetti, *New J. Phys.* **22**, 083085 (2020).
- [35] D. Farina, G. M. Andolina, A. Mari, M. Polini, and V. Giovannetti, *Phys. Rev. B* **99**, 035421 (2019).
- [36] F. Barra, *Phys. Rev. Lett.* **122**, 210601 (2019).
- [37] K. Ito and G. Watanabe, [arXiv:2008.07089](https://arxiv.org/abs/2008.07089).
- [38] J. Q. Quach and W. J. Munro, *Phys. Rev. Appl.* **14**, 024092 (2020).
- [39] A. Crescente, M. Carrega, M. Sassetti, and D. Ferraro, *New J. Phys.* **22**, 063057 (2020).
- [40] Q. Guo, C. Cheng, Z.-H. Sun, Z. Song, H. Li, Z. Wang, W. Ren, H. Dong, D. Zheng, Y.-Z. Zhang, R. Mondaini, H. Fan, and H. Wang, *Nat. Phys.* **17**, 234 (2021).
- [41] W.-B. He, S. Chesi, H.-Q. Lin, and X.-W. Guan, *Phys. Rev. B* **99**, 174308 (2019).
- [42] See Appendix for details.
- [43] E. T. Jaynes and F. W. Cummings, *Proc. IEEE* **51**, 89 (1963).
- [44] R. H. Dicke, *Phys. Rev.* **93**, 99 (1954).